

# The synthesis of SiC and TiC protective coatings for carbon fibers by the reactive replica process

R. Gadiou\*, S. Serverin, P. Gibot<sup>1</sup>, C. Vix-Guterl

*Institut de Chimie des Surfaces et Interfaces, UPR CNRS 9069, 15 rue Jean Starcky B.P. 2488, 68057 Mulhouse Cedex, France*

Received 16 August 2007; received in revised form 5 February 2008; accepted 8 February 2008

Available online 2 May 2008

## Abstract

The possibility to use the reactive replica technique to synthesize mono- and multi-layer coatings make it possible to cover carbon materials of complex shape by a ceramic layer. The reactive replica synthesis requires two steps: the deposition of an oxide layer on the carbon material by a sol–gel process, and a heat treatment above 1400 °C to form the carbide by reaction between the carbon material and the oxide layer. Several multi-layer coatings based on SiC and on SiC–TiC were synthesized by this process by using different carbon fibers. In this study, mono- and multi-layer carbide coatings were prepared on four different carbon fibers by the reactive replica technique to improve their resistance to oxidation between 500 and 1000 °C. The characteristics (surface area, thickness, . . .) of the carbide layers were studied in relation to the synthesis parameters such as the carbon surface properties, the nature of the carbide and the oxide thickness. The resistance to oxidation of the ceramic layers which can act as protective layers was studied between 500 and 1000 °C. The oxidation kinetics of the pristine and coated carbon fibers were studied in isothermal conditions by thermogravimetric analysis. It was observed that the surface of the pristine carbon fiber has a great influence on the efficiency of the protective coating. The thermogravimetric study showed that below 800 °C, the oxidation is controlled by the rate constant of the reaction either for non-coated or coated carbon fibers. Above this temperature, the oxidation rate is limited by the diffusion of oxygen through the coating layer. Moreover, the activation energy of the kinetic constant of the oxidation is not changed by the addition of the protective layer. This behaviour is an indication that the ceramic layer does not act as a diffusion barrier, the protection efficiency may be more related to the fact that the ceramic formation proceeds on the active sites of the carbon fibers, and therefore reduces its reactivity toward oxygen. The most effective protection against oxidation was obtained with a double layer of SiC. The addition of TiC in the protective layer either as a multi-layer of SiC and TiC or as a mono-layer of a mixture of the two carbides does not lead to any improvement of the protection efficiency against carbon oxidation. © 2008 Elsevier Ltd. All rights reserved.

**Keywords:** Sol–gel processes; Interfaces; Chemical properties; Carbon; SiC; TiC; Coatings

## 1. Introduction

The major drawback to the use of carbon fibers embedded or not in a ceramic matrix is their low oxidation resistance. Once the temperature is above 400 °C, the carbon fibers react with oxygen and rapidly burn away with an oxidation rate increasing quickly above 500 °C and with a reactivity which depends on their surface properties.<sup>1,2</sup> Such a drawback could be overcome by protecting the carbon by a ceramic matrix which acts as a diffusion barrier between oxygen and the carbon surface. Due

to the strategic importance of carbon-based composites in the aerospace industry, the development of such an effective oxidation protection system for carbon materials has been in progress for more than 50 years. Numerous materials have been studied to achieve this goal based on metals (Al, Ti) or non-metallic elements (Si, B). Ceramics have been widely used (carbides, nitrides),<sup>3–5</sup> but also oxides.<sup>6,7</sup> Among the numerous materials tested, SiC remains one of the most common ceramic matrix types due to its high melting point, excellent mechanical properties at high temperature, relatively good oxidation resistance up to 1500 °C in oxygen-rich atmospheres and stability in fast neutron environments. Moreover, SiC has the ability to form a SiO<sub>2</sub> layer in an oxidizing atmosphere which fills the cracks of the layer and increases the diffusion barrier efficiency.<sup>8</sup> Nevertheless, the efficiency of silica as a sealing agent is limited by its high viscosity. This problem has been partially addressed by

\* Corresponding author Tel.: +33 389 608 719, fax.: +33 389 608 799.  
E-mail address: [roger.gadiou@uha.fr](mailto:roger.gadiou@uha.fr) (R. Gadiou).

<sup>1</sup> Present address: Institut de Recherche Franco-Allemand, 5 rue du Général Cassagnou, 68300 Saint-Louis, France.

combining the SiC with other compounds leading to the design of innovative self-healing interphases and matrices.<sup>3,9–11</sup> By using this concept, multi-layered self-healing SiC-based matrices deposited by chemical vapour infiltration were built. Such coatings are constituted of binary or ternary phases forming fluid phases in oxidizing atmospheres that could fill the matrix cracks as soon as they are initiated and propagate under applied load in the material. As shown in the literature, the durability of these composites in severe environment is now good enough for applications in aeronautic engines.<sup>12</sup>

Beside the aeronautic and aerospace applications, new applications fields for the carbon fibers were targeted during these last years (heating elements in electrical furnace, IR lamp, . . .) for which the fiber must also be protected against oxidation or corrosion. However, for these low cost and wide-scale applications, the cost of the protection method of the fibers is a key parameter. Therefore, the classical way of ceramic deposition by chemical vapour deposition (CVD)<sup>3</sup> or reactive chemical vapour deposition (RCVD)<sup>13</sup> cannot be retained. SiC coating can also be directly prepared from a polysiloxane precursor but the final SiC layer obtained presents a cracked surface which does not prevent the oxygen diffusion.<sup>14</sup> To overcome these problems, we proposed in previous papers an alternative way based on a reactive templating procedure.<sup>15,16</sup> By this way, it is possible to obtain a carbon/carbide material which keeps the architecture of the initial carbon source and its flexibility. In this synthesis process, the carbon source is covered by an oxide layer prepared by a sol–gel process and the carbon/oxide artifact is further heat treated at temperature higher than 1200 °C to convert the oxide into a carbide. SiC materials with various textures (tubule, macroporous materials) as well as TiC coatings can be obtained by this way.<sup>17–19</sup> The sol–gel process has also been used to obtain other carbides like TiC or ZrC.<sup>4,19,20</sup> Another important advantage is that compared to the classical carboreduction by Acheson process, the sol–gel method makes it possible to synthesize carbide at lower temperature.<sup>21</sup>

In most cases, the overall reaction between the carbon and the oxide (carboreduction) reaction can be written as follows:



Nevertheless, the mechanism of the reaction depends on the final carbide formed. In the case of SiC, the reaction proceeds via two stages:

- A reaction between silica and carbon or between silica and silicon carbide leads to the formation of SiO through reaction (R2) and (R3):



Reaction (R2) will occur at the beginning of the reaction. Then, when the conversion yield increases, the interface between SiO<sub>2</sub> and carbon disappear and reaction (R3) becomes the main SiO formation path.

- SiO cannot undergo further reduction at the SiO<sub>2</sub>/SiC interface, so the only possibility is the diffusion of SiO in the SiC

layer and the formation of SiC at the C/SiC interface:



Previous studies have shown that the interfacial reactivity between silica and carbon and the morphology of the resulting SiC coating are influenced by the surface properties of the pristine carbon materials.<sup>16</sup>

In the case of the formation of titanium carbide, the conversion of TiO<sub>2</sub> into TiC proceeds through a multi-step mechanism<sup>22,23</sup>: the reaction involves the formation of intermediate oxides such as Ti<sub>3</sub>O<sub>5</sub> and Ti<sub>2</sub>O<sub>3</sub> with increasing temperature. The reaction proceeds then through the formation of titanium oxycarbides TiC<sub>x</sub>O<sub>y</sub> and finally TiC. Compared to SiC-based coatings, the use of TiC for protection of carbon materials against oxidation has not been extensively studied. The few studies which have been done on TiC coating of carbon fibers have shown that the efficiency of a TiC-based protective layer deposited by RCVD was lower than the one of SiC coatings.<sup>13</sup> The explanation for this behavior is that as TiC oxidizes at low temperature to give TiO<sub>2</sub> in a crystallized structure, the porosity of the carbide layer increases.

By using the reactive replica process, we can expect TiC coating layers which display different structural and textural properties. Previous studies done in our laboratory have shown that the use of a sol based on a mixture of SiO<sub>2</sub> and TiO<sub>2</sub> allows the synthesis of a carbide layer in which titanium and silicon carbide are homogeneously dispersed. Finally, a carbon material coated with a mixed SiC–TiC layer is obtained in which the crystallization of rutile particles is minimized.<sup>19,24</sup> The low temperature oxidation of such a mixed SiC–TiC layer should result in a mixture of components SiC–TiO<sub>2</sub> which could be a good protection against oxidation of carbon fibers.

Therefore, the use of the reactive templating process makes it possible to protect carbon fibers or cloth with a ceramic coating for which the textural and chemical properties and consequently the protection efficiency is strongly related to the surface characteristics of the carbon. To study the protection efficiency of such ceramic coatings, several mono- and multi-layers carbide coatings were deposited by the reactive replica process on carbon fibers which differ in terms of their surface characteristics. The protection efficiency of these coatings against carbon oxidation was tested in air between 500 and 1000 °C; temperatures higher than 1000 °C were not considered for the low cost applications targeted in this study. The oxidation kinetics of the carbon fibers with and without the coatings are discussed in relation with the characteristics of the ceramic coating, the ceramic–carbon interface and the characteristics of the carbon.

## 2. Experimental

### 2.1. Carbon fiber samples

Two types of carbon fibers were used: a polyacrylonitrile-based (PAN-based) carbon fiber and a viscose rayon-based carbon fiber. The main properties of the carbon fibers used for

Table 1  
Structural properties of the carbon fibers used for oxidation studies

Name	Precursor	Heat treatment (°C)	$L_C$ (Å)	$d_{002}$ (Å)	$I_D/I_G$	$L_a$ (Å)
R1600	ex-Rayon	1600	9	3.61	2.6	17
R2200	ex-Rayon	2200	21	3.46	0.4	109
P1500	ex-PAN	1500	16	3.50	4.0	11
P2000	ex-PAN	2000	52	3.41	1.6	27

this study are presented in Table 1. The first set of samples (R1600 and R2200) correspond to viscose rayon-based fibers heat treated at 1600 and 2200 °C, respectively. The second set of fibers are PAN-based carbon fibers. The samples named P1500 and P2000 correspond to a Celion fiber heat treated at 1500 °C and a Tenax high modulus fiber heat treated at 2000 °C, respectively.

The surface reactivity of carbon materials has often been correlated with its structural ordering. This last property is characterized by assuming that the carbon structure is based on small domains with a quasi-graphitic structure: the basic structural units (BSU). Therefore, the characterization of the structural ordering of carbon materials can be based on the properties of these BSU: their mean thickness,  $L_C$ , their mean size,  $L_a$ , and their crystallinity defined by the mean distance between the graphene layers,  $d_{002}$ . The structural ordering parameters of the carbon materials were determined by X-ray diffraction (XRD) performed with a X-Pert 2000 Philips instrument using Cu  $K\alpha_1$  radiation ( $\lambda = 0.154$  nm). The mean thickness of the crystallites  $L_C$  was obtained from the width and position of the 002 peak with the Sherrer formula, while the mean interlayer spacing between the graphene sheets  $d_{002}$  was computed from the position of the 002 peak with the Bragg formula.

In addition, Raman spectroscopy was done to characterize the structural ordering of the carbon fiber. The micro-Raman spectroscopy is well adapted to the characterization of graphitic carbon materials.<sup>25</sup> On hexagonal graphite, when the graphene layers are oriented normally to the incident beam, the vibrational G mode located around  $1580\text{ cm}^{-1}$  is the only one observed above  $100\text{ cm}^{-1}$  on the first order Raman spectrum. In disordered carbons, the D and D' bands located at  $1350$  and  $1620\text{ cm}^{-1}$ , respectively, are detected. They are assigned to defects within the carbon structure (edges, lattice defects or distorted graphene layers, ...). Both the band widths and band intensities can be used as structural improvement witnesses.<sup>26,27</sup> It has been observed by Tuinstra and Koenig<sup>28</sup> that the intensity ratio between the D and G bands  $R = I_D/I_G$  can be correlated to the inverse of the mean coherent domains ('crystallites') size:  $R = C(\lambda)/L_a$ . The value of the constant  $C$  depends on the wavelength of the laser used for Raman spectrometry  $\lambda$ . It should be mentioned that comparative studies between XRD and microprobe Raman technique have shown no strictly equivalent but rather complementary results.<sup>26,29</sup> The Raman spectra were recorded with a Jobin–Yvon micro-spectrometer coupled with a laser emitting at  $\lambda = 514.5$  nm, the green laser spot on the samples was about  $1\text{ m}^2$  with an incident power no higher than  $1\text{ mW}$  to prevent any sample from thermal degradation. With these experimental

conditions, we used a green laser ( $\lambda = 514$  nm) and the value of  $C$  is  $43.8\text{ Å}$ . The values of  $L_a$  obtained are presented in Table 1.

The data presented in Table 1 confirm as expected that the structural ordering of the carbon fiber increases with the heat-treatment. Nevertheless, the values of  $L_C$  shows that for a given temperature, PAN-based fibers display a higher degree of graphitization than rayon-based fibers. This behaviour is not observed for the values of  $L_a$ . The different evolution of these two parameters is related to the fact that  $L_C$  is measured by XRD and is a characterization of the bulk material, while  $L_a$  is measured by Raman spectrometry and is a surface parameter. Moreover,  $L_C$  describe the stacking of the graphene layers and is strongly dependant on the nature of the precursor and on the presence of heteroelements. Differences in the surface rugosity of the carbon fibers are observed by scanning electron microscopy (SEM) (see Fig. 1).

## 2.2. Synthesis of the protective coatings

The principle of the reactive replica method is summarized in Fig. 2. The nature of the oxide deposits on the carbon surface will depend on the final carbide targeted.  $\text{SiO}_2$ ,  $\text{TiO}_2$  and a mixed oxide  $\text{SiO}_2/\text{TiO}_2$  were prepared to obtain a layer of  $\text{SiC}$ ,  $\text{TiC}$  and a mixed carbide  $\text{SiC}/\text{TiC}$ , respectively. The oxide was prepared by a sol–gel process in which a liquid precursor is converted to the solid requested through chemical reactions (hydrolysis and polycondensation) at low temperatures.<sup>16</sup> This process has the advantage that it can be carried out at room temperature and pressure. Before the synthesis, the surfaces of the carbon fibers were desized by a thermal treatment at  $950\text{ °C}$  under argon during 15 h. The preparation of the sol has already been described elsewhere<sup>16,19</sup> and can be summarized as follow:

- $\text{SiO}_2$ : A solution of HCl (1 M), water and ethanol was added to a solution of tetraethyl-orthosilicate (TEOS)  $\text{Si}(\text{OC}_2\text{H}_5)_4$  in ethanol, the ratio of HCl (1 M):TEOS:ethanol:water was 0.4:1:4:10. The final solution was aged 30 min.
- $\text{TiO}_2$ : Acetylacetone diluted in butanol was added to a butanolic solution of  $\text{Ti}(\text{OC}_4\text{H}_9)_4$ , the volume ratio for acetylacetone:butanol:titanium butoxide was 1:6:2. The hydrolysis then was performed by adding a solution of HCl (1 M) and ethanol (volume ratio 2:3). The final solution was aged 30 min.
- $\text{SiO}_2\text{--TiO}_2$ : Two sols of Si and Ti were prepared according to the previous synthesis, and they were mixed with a ratio Si:Ti of 8:1.3.

Carbon fibers tows were then impregnated with the sol using a continuous dip-coating device: the impregnation time was 15 s. A drying was then carried on in air at room temperature during 30 min. The oxide layer was densified by a first thermal treatment up to  $1000\text{ °C}$  with a heating rate of  $5\text{ K/min}$ , followed by an isothermal step at  $1000\text{ °C}$  during 30 min. The final carbide layer was formed during a second thermal treatment at  $1450\text{ °C}$  with a heating rate of  $5\text{ K/min}$ . In order to record the reaction yield as a function of time and temperature, the different thermal treatments were done in a thermogravimetric apparatus (Setaram E 240) under an argon flow-rate. To avoid any secondary reac-

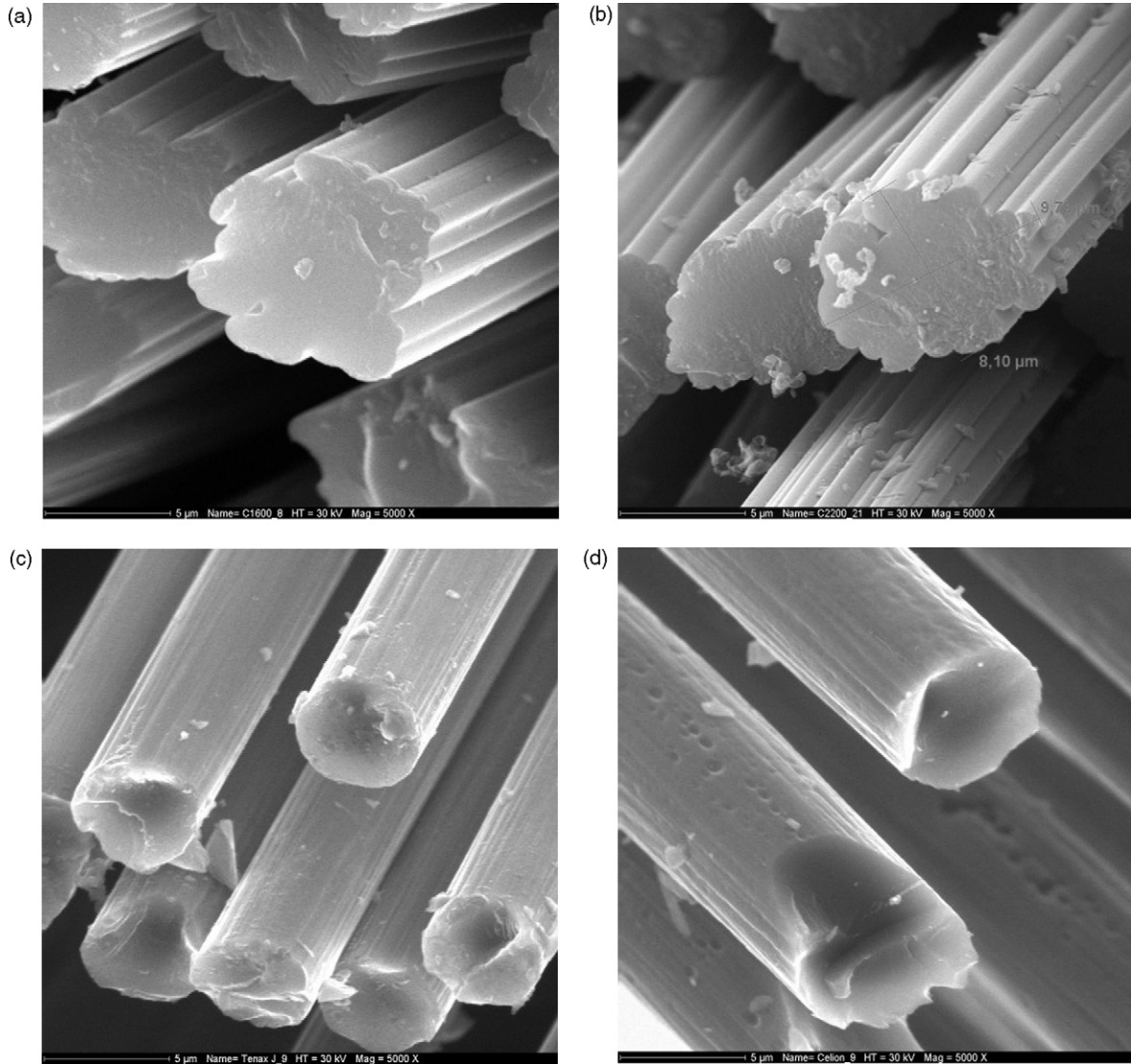


Fig. 1. SEM images of the pristine carbon fibers: (a) R1600, (b) R2200, (c) P1500 and (d) P2000. The size of the images is 20 μm × 20 μm.

tion with the sample holder, the carbon fibers were suspended in the reactor by a carbon wire. The overall carboreduction yield was determined by a three steps method:

- weighing of the C/MeC/MeO<sub>2</sub> composite;
- oxidation of the carbon at 600 °C in air and weighing of the MeC/MeO<sub>2</sub> composite;

- dissolution of the oxide with fluorhydric or sulfuric acid and weighing of the MeC material.

As pointed out in Section 1, multi-layer coatings have been proposed to increase the protective efficiency of the ceramic layer against carbon oxidation.<sup>30,31</sup> It then appeared interesting to study the influence of the coating thickness which can be

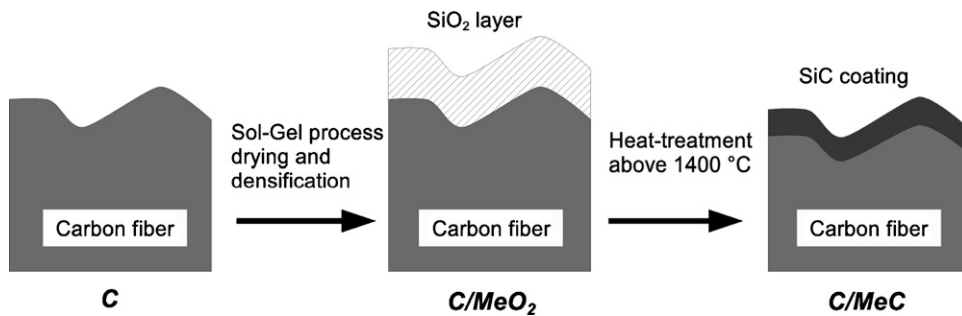


Fig. 2. Synthesis of carbides on carbon fiber surface by the reactive replica method.



controlled by doing successive impregnations and densification. Carbon fibers covered by a ceramic layer resulting from the formation of two successive SiC layers were prepared.

To characterize the ceramic coating formed, the carbon fibers were removed by a mild oxidation (at 600 °C) in dry air. The ceramic coating recovered was then characterized by XRD (Philips Xpert 2000 apparatus with the Cu K $\alpha$  wavelength at 1.54 Å), and by scanning electron microscopy.

In order to characterize the texture of the coatings, N<sub>2</sub> adsorption isotherms were done on the SiC layer after complete low temperature oxidation of the carbon. The total surface area  $S_{\text{BET}}$  was then computed with the BET method.<sup>32</sup>

### 2.3. Efficiency of protection against oxidation

The efficiency of the protection of the carbide layers was studied through the analysis of the kinetics of oxidation of the carbon fibers with and without the ceramic coating. This

study was done with a thermogravimetric apparatus Setaram E 240 under isothermal conditions. The sample was heated under a nitrogen gas flow at a heating rate of 5 K/min up to the desired temperature, that is between 500 and 950 °C, then the gas flow was switched to dry air. Typical curves are presented in Fig. 6. For all samples, the remaining mass of oxides and carbides was measured at the end of the oxidation, and the thermogravimetric curves were normalized to obtain the carbon burnoff. To evaluate the efficiency of the different coatings, the time to 50% of carbon burnoff  $t_{50}$  was used, and a protection index  $G$  was defined as the ratio of  $t_{50}$  for the coated carbon fibers to  $t_{50}$  for non-coated fibers.

## 3. Results and discussion

### 3.1. Characterization of the carbide coatings

SEM images of the coatings obtained with one or two layers of SiC are presented in Fig. 3a and b, respectively. We observed

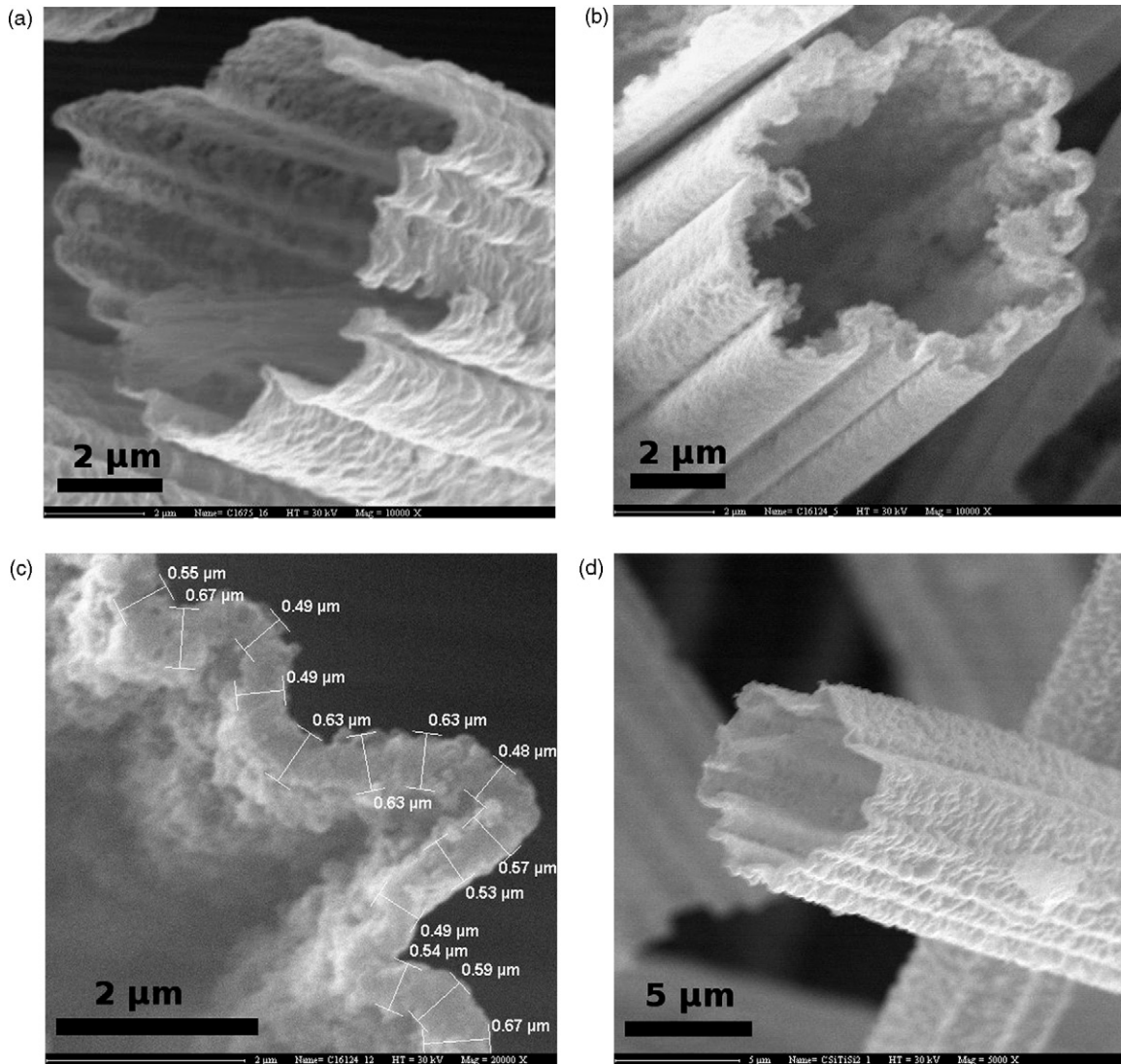


Fig. 3. MEB images of the ceramic coatings after a low temperature oxidation of the carbon fiber. The carbon fiber used was the R1600 sample with a final temperature of carboreduction equal to 1450 °C. (a) Mono-layer SiC coating, (b) double layer SiC-SiC coating, (c) detail of the double layer SiC-SiC coating showing the texture and the thickness of the layer and (d) double layer SiC-SiC/TiC coating.

Table 2  
Protection efficiency with mono-layer SiC coatings

Sample	$S_{\text{BET}}$ ( $\text{m}^2/\text{g}$ )	$G$
R1600/SiC	33	2.5
R2200/SiC	14	4
P1500/SiC	48	25
P2000/SiC	20	11

that the thickness of the SiC layer is twice the thickness of the mono-layer indicating that the conversion of  $\text{SiO}_2$  into SiC follows the same reaction mechanism after both  $\text{SiO}_2$  depositions. A surface area  $S_{\text{BET}}$  of the mono-layer coating equal to  $33 \text{ m}^2/\text{g}$  was measured. This value is far higher than the surface area of both the pristine carbon fibers which is below  $1 \text{ m}^2/\text{g}$ .

This result confirms the presence of an interconnected porosity in the SiC layer as confirmed by the SEM observations (see Fig. 3a), which shows the rugosity of the SiC layer. The mean thickness of the coating is close to  $0.2 \mu\text{m}$  for a mono-layer of SiC, and to  $0.5 \mu\text{m}$  for a double layer of SiC. It was observed that the nature of the carbon fibers (PAN-based or rayon-based) has no influence on the thickness of the SiC layer.

Fig. 5a present the XRD spectra of the R1600 mono-layer coating obtained at  $1450^\circ\text{C}$ : as expected b-SiC is obtained, and only traces of a-SiC were observed.<sup>33</sup> It must be also mentioned that the experimental conditions were chosen to obtain a total conversion of  $\text{SiO}_2$  into SiC; this was confirmed by the analysis on the SiC coating.

After removal of the carbon fibers by a mild oxidation, the specific surface area  $S_{\text{BET}}$  was determined and the results are reported in Table 2. These values show that a higher graphitization level of the pristine carbon fiber leads to a lower total surface area of the resulting SiC layer. The specific surface area of the carbide layer is mainly composed by the external surface of the elementary SiC grains. Therefore, this decrease of surface area shows that the SiC layers formed on highly ordered carbon materials R2200 and P2000 have a mean grain size which is higher than the one of R1600 and P1500. This is consistent with our previous results: when the carboreduction is done on a carbon fiber with a highly graphitized surface (i.e., with a low density of active sites), the first step of the reaction leads to a low number density of SiC nodules at the C/ $\text{SiO}_2$  interface, but these nodules have a large size.<sup>16</sup> The consequence is that the resulting carbide layers have a higher grain size and a lower surface area when they are synthesized on a carbon with a low surface reactivity.

If we compare the values presented in Table 2 with the structural data of the carbon fibers (Table 1), no direct correlation between the BET surface area of the SiC layer  $S_{\text{BET}}$  and the  $L_{\text{C}}$  parameter determined by XRD was observed. On the contrary, there is a direct correlation of  $S_{\text{BET}}$  with the ratio  $R = I_{\text{D}}/I_{\text{G}}$  computed from Raman spectra (Fig. 4). As pointed out above, this parameter characterizes the graphitization level of the carbon and quantitative correlations between  $R$  and the mean width of the crystallites  $L_{\text{a}}$  have been proposed.<sup>28</sup> This result confirms that an increase of the graphitization degree of the carbon surface leads to an increase of the grain size of the carbide layer and

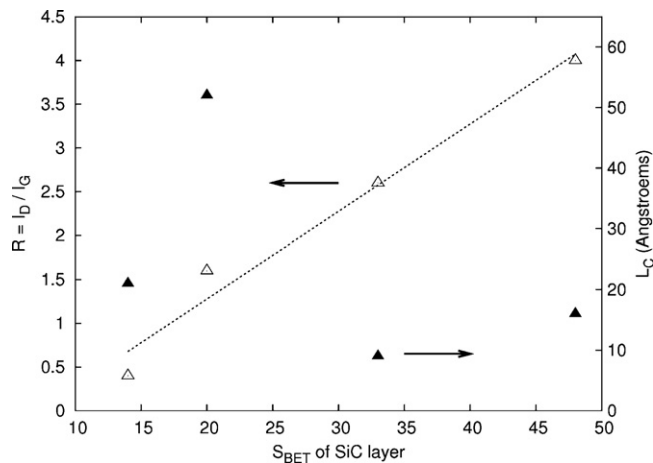


Fig. 4. Correlation of the surface area of the SiC layer with the structural parameters of the fibers (open triangles  $I_{\text{D}}/I_{\text{G}}$ , filled triangles  $L_{\text{C}}$ ).

consequently to a decrease of its surface area. It must be noticed also that  $S_{\text{BET}}$  is also correlated with the temperature of thermal treatment of the carbon fiber. The fact that the surface area is correlated with  $L_{\text{a}}$  and not with  $L_{\text{C}}$  is a consequence of the differences between the two parameters which have been highlighted above.  $L_{\text{C}}$  is a global characterization of the structural ordering of the bulk material, it is influenced by other chemical and structural parameters and it is therefore not directly related to the surface reactivity of the carbon material. On the contrary,  $L_{\text{a}}$  measured by Raman spectrometry is a true surface property. If we compare the BET surface areas in Table 2 with the values of  $L_{\text{C}}$  in Table 1, we can see that in a same family of carbon fibers (ex-PAN or ex-viscose) the surface area decreases when the structural ordering increases. This shows that  $L_{\text{C}}$  is correlated with the surface reactivity, but is also influenced by other bulk properties of the materials.

As pointed out in Section 1, the reactive replica synthesis was used to obtain mono- and multi-layer coatings based on TiC or on TiC–SiC mixtures. Previous studies done in our laboratory have shown that the carboreduction of a  $\text{SiO}_2/\text{TiO}_2$  gel does not lead to the formation of  $\text{Ti}_x\text{Si}_y\text{C}$  carbides but to a mixture of b-SiC and TiC.<sup>19</sup> Fig. 5b presents the XRD spectrum obtained with a single layer of TiC on P2000 fiber. Depending on the temperature, a solid solution of TiO and TiC can be formed,<sup>34,19</sup> the crystallographic patterns are similar for TiO and TiC but the presence of TiO leads to a decrease of the lattice parameter. In our experiments, the cell size was computed from the XRD patterns and we obtained a value of  $4.318 \text{ \AA}$  which is close to the value of TiC (i.e.,  $4.32 \text{ \AA}$ ).

### 3.2. Protection efficiency of the coatings

The isothermal oxidation of carbon fibers exhibits a sigmoidal profile, which is classical for this kind of material (see, for example, the curve R1600 in Fig. 6). This particular shape obtained in isothermal conditions shows that the oxidation of carbon fibers cannot be described by a simple mechanism with a reaction kinetic and a possible diffusion limitation. It proceeds through an autocatalytic mechanism: the beginning of the oxidation pro-

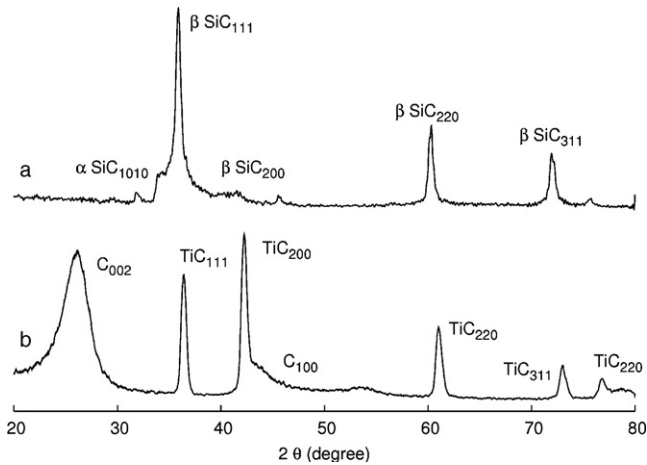


Fig. 5. XRD patterns of monolayer coatings: (a) SiC coating on R1600 sample (after oxidation of the carbon fiber) and (b) TiC coating on P2000 carbon fiber (with the carbon fiber present).

ceeds at low reaction rate, it is controlled by the kinetic law of the carbon–oxygen reaction. This step results in an increase of the surface area and of the active surface area. As a consequence, the sample reactivity increases and a maximum of the oxidation rate is observed for a carbon burnoff around 40–50%. Depending on the experimental conditions, the diffusion of oxygen in the boundary layer may limit the global oxidation rate during this second step. This behavior was already observed on ex-PAN fibers.<sup>35</sup>

The influence of the SiC coating on the oxidation kinetics of the R1600 material is also presented in Fig. 6. The values of  $G$  are 2.5 and 14 for mono- and double layers, respectively. We showed in the previous section that the thickness of the double carbide layer is twice the one of the mono-layer coating. Therefore, this increase in protection efficiency seems to be related to the increased thickness of the SiC layer. Another parameter which is improved in the double layer is the specific surface area: 15 m<sup>2</sup>/g compared to 33 m<sup>2</sup>/g for a mono-layer of silicon carbide. These observations shows that the increase of the layer

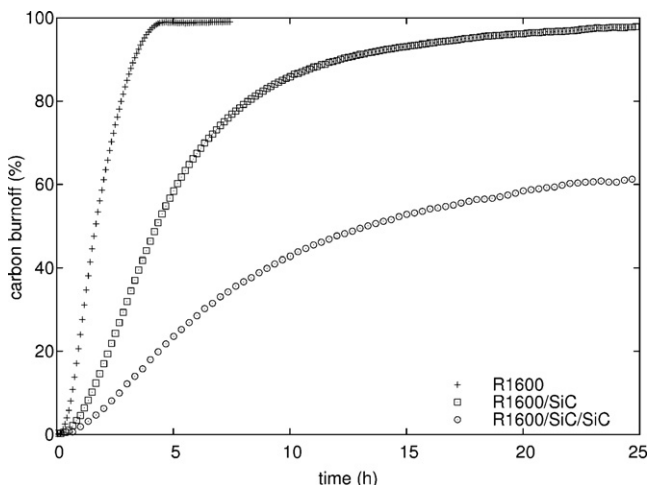


Fig. 6. Influence of mono and double layer of SiC coating on the oxidation profiles of R1600 material at 600 °C.

thickness leads to an increase of the efficiency as a diffusion barrier. Nevertheless, the shape of the carbon burnoff profile shows that the global reaction rate is controlled by the kinetic law of the C–O<sub>2</sub> reaction even for a double layer coating. This observation suggests that the diffusion of oxygen through the protective layer is not the limiting process of the oxidation. The correlation between the layer thickness, the surface area and the protection efficiency is therefore not simple.

The TGA curves obtained at different temperatures between 500 and 950 °C were analyzed with the Avrami–Erofeev model.<sup>36,37</sup> This model was initially developed for phase changes. It assumes that the onset of the oxidation takes place on nuclei dispersed on the sample. Then the reaction leads to an increase of the reaction sites and therefore an increase of the reaction rate is observed. Following this model, the relation which is expected between the reaction yield and the time is:

$$\tau = 1 - \exp(-(kt)^n) \quad (1)$$

in which  $\tau$  is the conversion yield,  $t$  the time,  $k$  the rate constant and  $n$  the reaction order. The value of  $n$  is 2 or 3 if the nucleation is a 2D or 3D process, the sigmoid shape of the thermograms is characteristic of this kind of mechanism. In its study on PAN-based carbon fiber oxidation, Gao et al.<sup>35</sup> obtained a best fit between the experimental data and the model for an order  $n = 1$ . In our case with rayon-based carbon fibers, the best agreement was obtained for  $n = 2$ . An example of fitting for the isothermal oxidation of the sample R1600 at 600 °C is presented in Fig. 7.

From these experiments, we were able to obtain the values of  $k$  as a function of the oxidation temperature. Fig. 8 present the Arrhenius plot of these values for the sample R1600 without and with a SiC mono-layer coating. From the low temperature values measured between 500 and 800 °C, an activation energy of 128 kJ/mole can be computed. This value is of the same order although somewhat lower than values already presented in the literature.<sup>38,35</sup> Above 800 °C, the influence of temperature on the overall reaction rate becomes very low. This is the typical behavior which is observed when an heterogeneous reaction becomes partially or totally controlled by the diffusion of the reactants

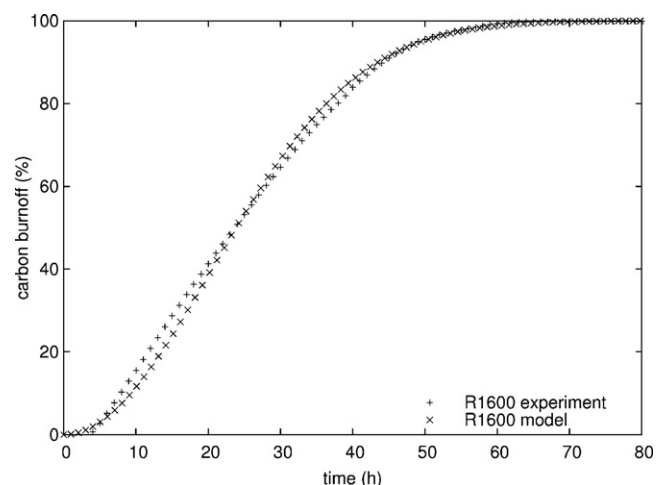


Fig. 7. Comparison between experimental and simulated thermograms for the oxidation of R1600 sample at 600 °C.



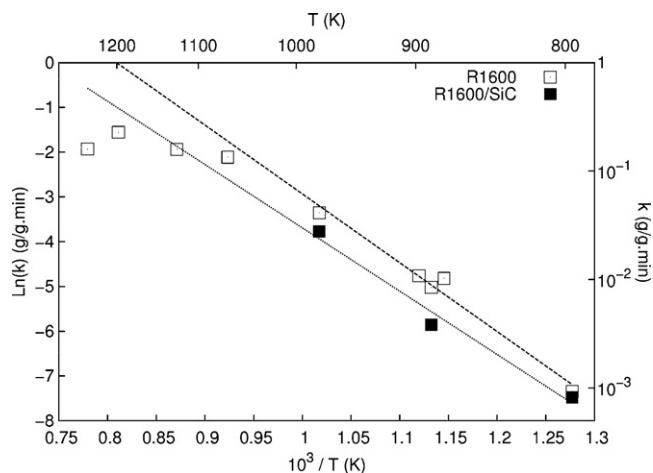


Fig. 8. Arrhenius plot of oxidation kinetics for R1600 fiber and for R1600 fiber coated with a mono-layer of SiC.

from the gas phase to the surface. The influence of temperature on diffusion coefficients is indeed very low compared to the exponential form of the Arrhenius law. Then, it is obvious from the values presented in Fig. 8 that above 800 °C, the reaction is limited by the diffusion of oxygen. This leads to an important decrease of the apparent activation energy of the process.

In Fig. 8, the rate constants for the oxidation of carbon fibers R1600 protected by a mono-layer of SiC are also presented. Whatever the temperature, a significant decrease of the oxidation rate is observed. We can see also that the influence of the temperature on the oxidation rate is the same for the pristine and the protected carbon materials. As a consequence, the activation energy for the oxidation of R1600 fiber coated by a SiC mono-layer is 117 kJ/mole which is close to the value of the non-coated carbon fiber. If the SiC layer would be a diffusion barrier for oxygen, the oxidation rate would be at least partially controlled by the diffusion of oxygen through the carbide layer. As the influence of temperature on diffusion coefficients is low, this should result in a significant decrease of the apparent activation energy of the global oxidation kinetic law. In regard to these results, another mechanism related to the active sites presents on the carbon surface can be proposed. The density of active sites at the surface of a carbon material is a key parameter for the characterization of its reactivity toward oxidants.<sup>39</sup> As discussed previously in Section 3.1, the active sites play an important role in the formation of the SiC layer.<sup>17,16</sup> Hence, the nucleation of the SiC aggregates begins on the active sites of the carbon fiber which become no longer available for any interaction with a gaseous environment. These active sites are no longer available for the reaction with oxygen and as a consequence, a significant decrease of the oxidation rate is observed.

Compared to rayon-based carbon fibers, the oxidation of ex-PAN fibers does not proceed through an auto-accelerating kinetic mechanism (Fig. 9). Therefore, the best fitting with an Avrami–Erofeev law was obtained for  $n=1$ . This is in good agreement with the results obtained by Gao et al. on three-dimensional braided carbon fibers.<sup>35</sup> Fig. 9 also presents the influence of a mono-layer SiC coating on the oxidation rate of two ex-PAN fibers. As for ex-rayon fibers, the shape of the oxi-

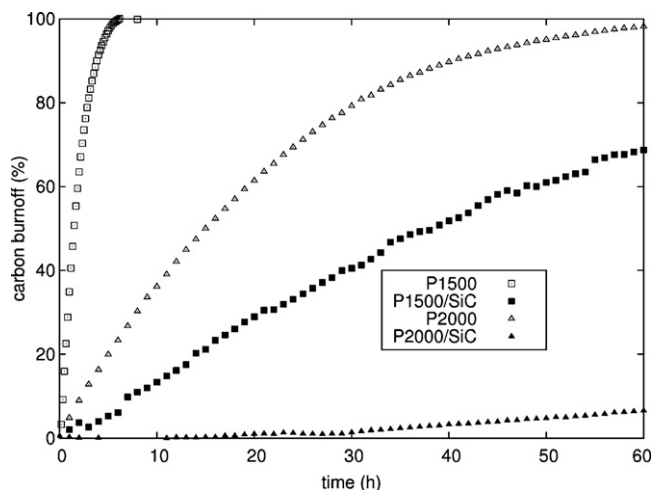


Fig. 9. Protection efficiency of a mono-layer of SiC on ex-PAN fibers. The burnoff curves were recorded in isothermal conditions at 600 °C in air.

dation curve is not modified by the presence of the SiC coating although the overall oxidation rate is significantly decreased. This shows that for ex-PAN fibers the protection effect of the carbide layer is not related to a change in the mechanism of oxidation.

The  $G$  values in Table 2 also shows that the protection efficiency is better for PAN-based fiber than for rayon-based fibers. These higher values of  $G$  are obtained although the surface area of the SiC layers seems to be significantly higher. This confirms that the SiC layer does not operate as a diffusion barrier in this oxidation temperature range.

We have synthesized mixed TiC–SiC coating with a molar ratio Si/Ti of 8 on R1600 sample and compared the obtained protection efficiency with the ones of SiC layers. Two synthesis pathways have been used:

- The carboreduction of a mixed sol–gel of silica and titanium oxide (sample R1600/SiC–TiC).
- The synthesis of coatings with two successive layers: the first one with a mixture SiC–TiC and the second one with TiC (sample R1600/SiC–TiC/SiC).

The influence of SiC–TiC coatings on isothermal oxidation of R1600 carbon fiber is presented in Fig. 10. As for the SiC coatings, the addition of a titanium carbide layer on rayon-based carbon fibers does not lead to any changes in the mechanism of oxidation: a sigmoidal shape of the thermograms is observed for all samples. Moreover, the addition of titanium carbide to the SiC coating does not lead to a significant improvement of the protection efficiency: the value of  $G$  are 2.5 and 2 for the layers without TiC (R1600/SiC) or with TiC (R1600/SiC–TiC), respectively. The addition of a second layer of SiC on the SiC–TiC coating improves somewhat the protection index  $G$  up to 2.5, but this value is far lower than the one obtained with a double SiC/SiC layer ( $G=14$ ).

Therefore, it can be concluded that the addition of TiC leads to a decrease of the protection efficiency of the carbide coatings. This trend is not related to the porosity of the carbide layer: the



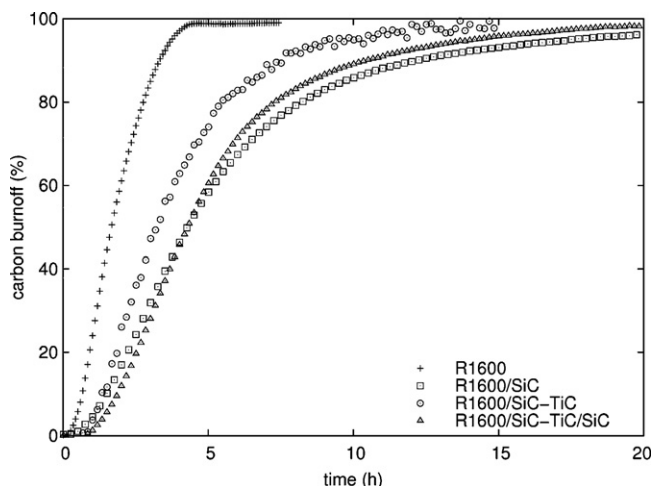


Fig. 10. Protection efficiency of coatings based on SiC–TiC mixtures on ex-rayon fibers. The burnoff curves were recorded in isothermal conditions at 600 °C in air.

BET surface area of the SiC–TiC coating is 22 m<sup>2</sup>/g, which is significantly lower than the value observed for a mono-layer of SiC ( $S_{\text{BET}} = 33 \text{ m}^2/\text{g}$ ). Therefore, the higher oxidation rate observed for carbon fibers coated with SiC–TiC is not related to a higher diffusion rate of oxygen through the ceramic layer. This confirms again that in this temperature range, the coating does not operate as a diffusion barrier.

#### 4. Conclusions

The reactive replica process makes it possible to synthesize carbide coatings on carbon materials with complex shapes. Moreover, the composition (SiC, TiC or SiC–TiC mixtures) and the thickness of the coating layer can be tailored by a judicious choice of the experimental conditions and the carbide precursors. We were able to obtain mono- and multi-layer coatings of SiC and TiC with a thickness ranging between 0.2 and 0.5 μm. It was observed that the texture of the coating layer is strongly correlated with the structural ordering of the surface.

These ceramic layers were used as a protection against oxidation for PAN-based and rayon-based carbon fibers between 600 and 1000 °C. A study of the influence of temperature on the oxidation rate of rayon-based carbon fiber with or without a SiC coating was done. It was shown that the activation energy of the kinetic of oxidation for the protected carbon fiber is similar to the one of the pristine material, and its relatively high value is an indication that the oxidation is not controlled by the diffusion of oxygen through the carbide layer. The fact that the oxidation rate is not correlated with the porosity of the layer supports this assumption. It seems that the carbide formation takes place on the active sites of the carbon surface, this leads to a decrease of its intrinsic reactivity toward oxidants. A key point for this process is that the improvement of the resistance to oxidation depends on the structural properties of the pristine carbon surface. The surface influences both the kinetic of the oxidation and the properties of the coating layer formed by the sol–gel process.

We show in this paper that a 0.2 μm SiC coating on the carbon fibers leads to a significant decrease of the oxidation rate. The best protection efficiency was achieved with a double layer of silicon carbide, which leads to a decrease of the oxidation of the rayon-based carbon fiber at 600 °C by a factor 14. Therefore, this low cost and simple synthesis process is attractive to obtain efficient protection layers on carbon fibers or clothes.

#### Acknowledgment

This work was supported by a ‘Performance’ grant of the French Ministry of Industry.

#### References

- Luthra, K. L., Oxidation of carbon/carbon composites—a theoretical analysis. *Carbon*, 1988, **26**(2), 217–224.
- Ehrburger, P., Lahaye, J. and Bourgeois, C., Characterization of carbon–carbon composites—II: oxidation behaviour. *Carbon*, 1981, **19**(1), 7–10.
- Labruquere, S., Blanchard, H., Pailler, R. and Naslain, R., Enhancement of the oxidation resistance of interfacial area in C/C composites. Part I: Oxidation resistance of B–C, Si–B–C and Si–C coated carbon fibres. *J. Eur. Ceram. Soc.*, 2002, **22**(7), 1001–1009.
- Vix-Guterl, C., Serverin, S., Gibot, P. and Gadiou, R., Protective ceramic multilayer coatings for carbon materials obtained by a reactive templating procedure. In *IX Conference & Exhibition of the European Ceramic Society*, 2005.
- Gao, P. Z., Wang, H. J. and Jin, Z. H., Oxidation kinetics and mechanism of SiC coating/3-dimensional carbon fiber braid. *J. Inorg. Mater.*, 2005, **20**(2), 323–331.
- Wang, Y.-Q., Zhou, B.-L. and Wang, Z.-M., Oxidation protection of carbon fibers by coatings. *Carbon*, 1995, **33**(4), 427–433.
- Vix-Guterl, C. and Ehrburger, P., *World of Carbon, ‘Fibers and Composites’*, vol. 2. Taylor and Francis, London, 2003, p. 188.
- Gadiou, R., Serverin, S. and Vix-Guterl, C., A thermogravimetric study of the influence of carbides multi-layers coatings on carbon fibers oxidation. In *Int. Conference on Carbon 2005*, 2005.
- Vincent, H., Vincent, C., Scharff, J. P., Mourichoux, H. and Bouix, J., Thermodynamic and experimental conditions for the fabrication of a boron carbide layer on a high modulus carbon fiber surface by RCVD. *Carbon*, 1992, **30**, 495–505.
- Qian-Gang, F., He-Jun, L., Xiao-Hong, S., Ke-Zhi, L., Chuang, W. and Min, H., Double-layer oxidation protective SiC/glass coatings for carbon/carbon composites. *Surf. Coat. Technol.*, 2006, **200**(11), 3473–3477.
- Qian-Gang, F., He-Jun, L., Xiao-Hong, S., Ke-Zhi, L., Jian, W. and Min, H., Oxidation protective glass coating for SiC coated carbon/carbon composites for application at 1773 K. *Mater. Lett.*, 2006, **60**(3), 431–434.
- Naslain, R., Design, preparation and properties of non-oxide CMCs for application in engines and nuclear reactors: an overview. *Compos. Sci. Technol.*, 2004, **64**(2), 155–170.
- Piquero, T., Vincent, H., Vincent, C. and Bouix, J., Influence of carbide coatings on the oxidation behavior of carbon fibers. *Carbon*, 1995, **33**, 455–467.
- Kern, F. and Gadov, R., Deposition of ceramic layers on carbon fibers by continuous liquid phase coating. *Surf. Coat. Technol.*, 2004, **180**181, 533537.
- Vix-Guterl, C., Alix, I., Gibot, P. and Ehrburger, P., Formation of tubular silicon carbide from a carbon-silica material by using a reactive replica technique: infra-red characterisation. *Appl. Surf. Sci.*, 2003, **210**, 329–337.
- Vix-Guterl, C., Alix, I. and Ehrburger, P., Synthesis of tubular silicon carbide (SiC) from a carbonsilica material by using a reactive replica technique: mechanism of formation of SiC. *Acta Mater.*, 2004, **52**, 1639–1651.

17. Vix-Guterl, C. and Ehrburger, P., Effect of the properties of a carbon substrate on its reaction with silica for silicon carbide formation. *Carbon*, 1997, **35**(10–11), 1587–1592.
18. Vix-Guterl, C., Mac Enaney, B. and Ehrburger, P., SiC material produced by carbothermal reduction of a freeze gel silica–carbon artefact. *J. Eur. Ceram. Soc.*, 1999, **19**, 427–432.
19. Gibot, P. and Vix-Guterl, C., TiO<sub>2</sub> and TiO<sub>2</sub>/β-SiC microtubes prepared from an original process. *J. Eur. Ceram. Soc.*, 2007, **27**(5), 2195–2201.
20. Rambo, C., Cao, J., Rusina, O. and Sieber, H., Manufacturing of biomorphic (Si, Ti, Zr)-carbide ceramics by sol–gel processing. *Carbon*, 2005, **43**(6), 1174–1183.
21. Kurokawa, Y., Ota, H. and Sato, T., Preparation of carbide fibres by thermal decomposition of cellulose-metal (Ti, Zr) alkoxide gel fibres. *J. Mater. Sci. Lett.*, 1994, **13**(7), 516–518.
22. Koc, R., Kinetics and phase evolution during carbothermal synthesis of titanium carbide from ultrafine titania/carbon mixture. *J. Mater. Sci.*, 1998, **33**(4), 1049–1055.
23. Gibot, P., Elaboration and characterization of ceramic materials SiC, TiC and SiC/TiC with a controlled morphology by the reactive replica method (in French). Ph.D. thesis. University of Mulhouse, 2002.
24. Pierre, A. C., *Introduction to Sol–Gel Processing*. Kluwer Academic Publishers, London, 1998.
25. Holden, J. M., Jishi, R. A. and Eklund, P. C., Vibrational modes of carbon nanotubes, spectroscopy and theory. *Carbon*, 1995, **33**(7), 959–972.
26. Rouzaud, J.-N., Oberlin, A. and Beny-Bassez, C., Carbon films: structure and microtexture (optical and electron microscopy, Raman spectroscopy). *Thin Solid Films*, 1983, **105**(1), 75–96.
27. Beyssac, O., Goffe, B., Petitet, J.-P., Froigneux, E., Moreau, M. and Rouzaud, J.-N., On the characterization of disordered and heterogeneous carbonaceous materials by Raman spectroscopy. *Spectrochim. Acta A: Mol. Biomol. Spectrosc.*, 2003, **59**(10), 2267–2276.
28. Tuinstra, F. and Koenig, J. L., Raman spectrum of graphite. *J. Chem. Phys.*, 1970, **53**(3), 1126–1130.
29. Cuesta, A., Dhameincourt, P., Laureyns, J., Martínez-Alonso, A. and Tascón, J. M. D., Comparative performance of X-ray diffraction and Raman microprobe techniques for the study of carbon materials. *J. Mater. Chem.*, 1998, **8**, 2875–2879.
30. Wunder, V., Popovska, N., Wegner, A., Emig, G. and Arnold, W., Multilayer coatings on CFC composites for high temperature applications. *Surf. Coat. Technol.*, 1998, **101–102**, 329–332.
31. Huang, J.-F., Li, H.-J., Zeng, X.-R. and Li, K.-Z., Preparation and oxidation kinetics mechanism of three-layer multi-layer-coatings-coated carbon/carbon composites. *Surf. Coat. Technol.*, 2006, **200**(18–19), 5379–5385.
32. Rouquerol, F., Rouquerol, J. and Sing, K., *Adsorption by Powders and Porous Solids—Principles, Methodology and Applications*. Academic Press, London, 1999, p. 54, Chapter 3.
33. Huang, J.-F., Zeng, X.-R., Li, H.-J., Xiong, X.-B. and Fu, Y.-W., Influence of the preparation temperature on the phase, microstructure and anti-oxidation property of a SiC coating for C/C composites. *Carbon*, 2004, **42**(8–9), 1517–1521.
34. Koc, R. and Folmer, J. S., Carbothermal synthesis of titanium carbide using ultrafine titania powders. *J. Mater. Sci.*, 1997, **V32**(12), 3101–3111.
35. Gao, P., Wang, H. and Jin, Z., Study of oxidation properties and decomposition kinetics of three-dimensional (3-D) braided carbon fiber. *Thermochim. Acta*, 2004, **414**(1), 59–63.
36. Avrami, M., Granulation, phase change, and microstructure kinetics of phase change—III. *J. Chem. Phys.*, 1941, **9**, 177–184.
37. Erofeev, B. V., Generalized equation of chemical kinetics and its application in reactions involving solids. *C. R. Acad. Sci. USSR*, 1946, **52**, 511–518.
38. Labruquere, S., Blanchard, H., Pailler, R. and Naslain, R., Enhancement of the oxidation resistance of interfacial area in C/C composites. Part II: Oxidation resistance of B–C, Si–B–C and Si–C coated carbon preforms densified with carbon. *J. Eur. Ceram. Soc.*, 2002, **22**(7), 1011–1021.
39. Ehrburger, P., Louys, F. and Lahaye, J., The concept of active sites applied to the study of carbon reactivity. *Carbon*, 1989, **27**(3), 389–393.